Experimental preparation of two-photon Knill-Laflamme-Milburn states

Karel Lemr,[1] Antonín Černoch,[1] Jan Soubusta,[1] and Jaromír Fiurášek[2]

[1]*Joint Laboratory of Optics of Palacký University and Institute of Physics of Academy of Sciences of the Czech Republic, 17. listopadu 50A, 779 07 Olomouc, Czech Republic*

[2]*Department of Optics, Palacký University, 17. listopadu 12, 771 46 Olomouc, Czech Republic*

(Received 26 October 2009; published 22 January 2010)

We report an experimental preparation of the so-called Knill-Laflamme-Milburn states (KLM states) that have been known to have interesting properties related to quantum information processing. Our experiment has demonstrated successful preparation of entangled two-photon four-mode KLM states using spontaneous parametric down-conversion as a source of entangled photon pairs, linear optical components, and avalanche photodiodes for single-photon detection. We have verified the successful generation of KLM states by complete quantum state tomography.

DOI: 10.1103/PhysRevA.81.012321 PACS number(s): 03.67.Bg, 42.50.Dv, 42.50.Ex

I. INTRODUCTION

The formulation of basic principles of quantum physics at the beginning of the twentieth century has been quickly succeeded by exploration of possible applications of the discovered quantum properties of matter and light. During recent years, theoretical and experimental effort among other fields of interest aimed at enriching classical information processing by joining it with the quantum theory and thus developing quantum information processing (QIP) [1,2]. It was demonstrated that QIP surpasses classical information processing in several ways. For instance, quantum cryptography offers an inherent security to cyphered communications due to the fundamental property of quantum states known as the no-cloning theorem [3–5]. Other examples include the significant improvement in efficiency of several computational algorithms such as factorizing [6–9].

Light is a particularly suitable quantum information carrier [10]. Moreover, a universal quantum computation can be in principle carried out using only linear optical elements such as beam splitters or phase shifters, single-photon sources, and single-photon detectors [11]. Triggered by this seminal discovery, a significant amount of theoretical and experimental work has been devoted to the development of basic linear-optical quantum gates [11–16] and related technologies [17,18] with the ultimate goal of constructing an optical quantum computer in the future.

One of the major setbacks of QIP with light is the probabilistic nature of almost all of the QIP schemes. Typically, the success probability decreases with increasing complexity of the scheme. However, as shown by Knill, Laflamme, and Milburn this disadvantage may be overcome by employing a specific class of ancillary entangled multiphoton states (referred to as KLM states) that may reduce the failure probability of linear optical quantum gates to an arbitrarily small value inversely proportional to the size of the multiphoton KLM state [11]. Besides the capability of increasing the success probability of complex quantum computational schemes, the KLM states have been known to enhance other QIP tasks as well. Even the two-photon KLM states can be employed to perform quantum state teleportation and error correction [19].

In this paper we report on an experimental generation and full characterization of the entangled two-photon KLM states. Our experiment follows a recent theoretical proposal by two of the present authors [20] who showed that spontaneous parametric down-conversion (SPDC) along with linear optical components is sufficient to prepare the two-photon KLM states in a more general form put forward by Franson *et al.* [13],

$$|\psi_{\mathrm{KLM}}\rangle = \gamma|1100\rangle + \delta|1001\rangle - \gamma|0011\rangle. \tag{1}$$

Here γ and δ are real numbers satisfying $2\gamma^2 + \delta^2 = 1$ and 0 and 1 denote the number of photons in the first through fourth spatial mode. It is easy to see that by means of polarizing beam splitters the state (1) can be transformed into a state of two spatial modes and two polarization modes,

$$|\psi_{\mathrm{KLM}}\rangle = \gamma|H_1V_1\rangle + \delta|H_1V_2\rangle - \gamma|H_2V_2\rangle, \tag{2}$$

where $|H\rangle$ and $|V\rangle$ denote states of a single photon with horizontal and vertical linear polarization, respectively, and subscripts 1 and 2 label the two spatial modes.

II. EXPERIMENTAL SETUP

Our experimental setup for generation and characterization of the states (2) is shown in Fig. 1. It can be divided into three main parts: source of entangled photon pairs, KLM state preparation, and KLM state analysis. To generate an entangled two-photon state, we use a pair of beta barium borate (BBO) type I ($e \rightarrow oo$) nonlinear crystals with orthogonally rotated phase-matching planes as proposed by Kwiat *et al.* [21] [see Fig. 1(a)]. The optical pumping is supplied by a cw krypton-ion laser at the wavelength of 413.1 nm and about 200 mW of optical power. Before impinging on the crystal, the pumping beam passes through a half-wave plate (HWP) and a quarter-wave plate (QWP) so that we can set arbitrary polarization of the beam. Nonlinear processes of SPDC ($H \rightarrow VV$) and ($V \rightarrow HH$) are occurring coherently and simultaneously in the first and the second crystal, respectively. Because of the fact that these two processes are indistinguishable, the resulting state of the emitted photon pairs can be expressed as a coherent superposition of two terms,

$$|\Phi_1\rangle = \sin\alpha|H_1H_2\rangle + \mathrm{e}^{i\phi}\cos\alpha|V_1V_2\rangle, \tag{3}$$

where subscripts 1 and 2 label the spatial modes. Parameters α and ϕ can be controlled by rotation of the HWP and tilt of the QWP in the pump beam.

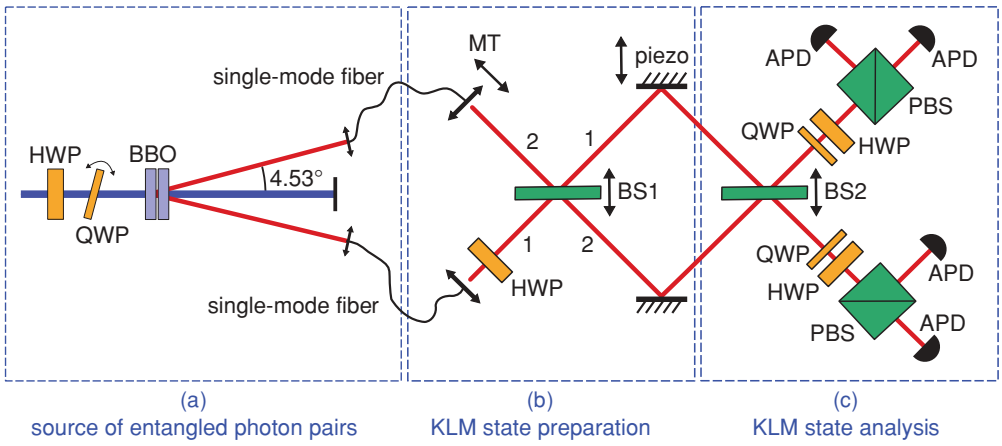

FIG. 1. (Color online) Experimental setup divided into three main parts: (a) source of entangled photon pairs, (b) KLM state preparation, and (c) KLM state analysis. Optical components are labeled as follows: HWP, half-wave plate; QWP, quarter-wave plate; BBO, nonlinear crystals; MT, motorized translation; BS, beam splitter; PBS, polarizing beam splitter; APD, set of cut-of filter, single-mode fiber, and avalanche photodiode. Spatial modes are labeled 1 and 2, respectively.

Photons in the state (3) are transferred by two single-mode optical fibers to the entrance of the second part of our setup—the KLM state preparation [see Fig. 1(b)]. The single-mode fibers serve also as spatial mode filters, allowing us to reach high interference visibility. First, we swap the polarization of one photon of the pair by putting a diagonally rotated HWP into its path. The resulting state reads

$$|\Phi_2\rangle = \sin\alpha|V_1H_2\rangle + e^{i\phi}\cos\alpha|H_1V_2\rangle. \tag{4}$$

Subsequently, the photons are coherently superposed on the beam splitter BS1. Both beam splitters BS1 and BS2 are attached to a microtranslation and can be transversally shifted as depicted by the arrows. The path of the reflected beam depends strongly on the beam splitter positioning, while the transmitted beam is left almost unaffected. By shifting the beam splitter we are thus able to tune its effective reflectivity/transmissivity ratio in the range from 50:50 to 0:100. This operation can be expressed as a linear transformation of the annihilation operators,

$$\begin{aligned}\hat{a}_{1,\mathrm{out}} &= \frac{1}{\sqrt{2}}(\hat{a}_{1,\mathrm{in}} + \sigma\hat{a}_{2,\mathrm{in}} + \sqrt{1-\sigma^2}\,\hat{a}_{1,\mathrm{vac}}),\\ \hat{a}_{2,\mathrm{out}} &= \frac{1}{\sqrt{2}}(\hat{a}_{2,\mathrm{in}} - \sigma\hat{a}_{1,\mathrm{in}} + \sqrt{1-\sigma^2}\,\hat{a}_{2,\mathrm{vac}}),\end{aligned} \tag{5}$$

where $\hat{a}_{j,\mathrm{vac}}$ denote annihilation operators of auxiliary vacuum modes. The effective amplitude reflectance $\sigma \in [0;1]$ is set by the position of the beam splitter on the microtranslation and can be adjusted as needed. After the interference on BS1 the state conditioned on the presence of both photons in the signal output modes reads

$$\begin{aligned}|\Phi_3\rangle = \tfrac{1}{2}[&\sigma(\sin\alpha + e^{i\phi}\cos\alpha)(|H_1V_1\rangle - |H_2V_2\rangle)\\ &+ (\sin\alpha - \sigma^2 e^{i\phi}\cos\alpha)|V_1H_2\rangle\\ &+ (e^{i\phi}\cos\alpha - \sigma^2\sin\alpha)|H_1V_2\rangle].\end{aligned} \tag{6}$$

To prepare the KLM state (2) one needs to nullify the amplitude of the undesired term $|V_1H_2\rangle$. This can be achieved by setting $\phi = 0$ and $\sigma = \sqrt{\tan\alpha}$. This choice ensures that the resulting state (6) becomes equivalent to the required KLM state (2) with real parameters γ and δ satisfying

$$\frac{\gamma}{\delta} = \frac{\sqrt{\sin\alpha\cos\alpha}}{\cos\alpha - \sin\alpha}. \tag{7}$$

From this equation we can determine α for any target ratio γ/δ that fully specifies the KLM state (2).

We begin the experiment by performing the photon source adjustment. Beam splitters BS1 and BS2 are shifted to the 0:100 ($\sigma = 0$) position during this phase so that we can perform the quantum state tomography and estimation [22] of the state $|\Phi_2\rangle$ generated by the crystal. This tomography determines the values of α and ϕ, which can be adjusted by rotation of the HWP and the tilt of the QWP in the pump beam. We have obtained high state purity of about 94%–98% and fidelity of about 94%. After the adjustment of the photon source is complete, we put the beam splitter BS1 into position so that $\sigma = \sqrt{\tan\alpha}$. Motorized translation MT is then used to balance the lengths of photon trajectories to maximize the visibility of Hong-Ou-Mandel (HOM) interference [23] on the beam splitter BS1 where the KLM state is created.

III. STATE ANALYSIS

The state analysis is performed in three basic steps using part c of the experimental setup. For the purposes of the first two ones the beam splitter BS2 is tuned to the 0:100 position (and so it can be considered as effectively removed). The third step of the analysis requires the beam splitter BS2 to be placed also into the 50:50 ($\sigma = 1$) position.

In the first analysis step we verify that the undesired term H_2V_1 vanishes due to destructive two-photon interference on BS1. This can be achieved by measuring the coincidences for different positions of the motorized translation (see Fig. 2). The experimental data clearly show that the H_2V_1 coincidences realize dip with typical visibility around 95% and they represent only about 0.45% of the total signal at the dip. In order to confirm that the prepared state is not contaminated by other unwanted contributions we have further measured the coincidences H_1H_2 and V_1V_2, which turned out to be

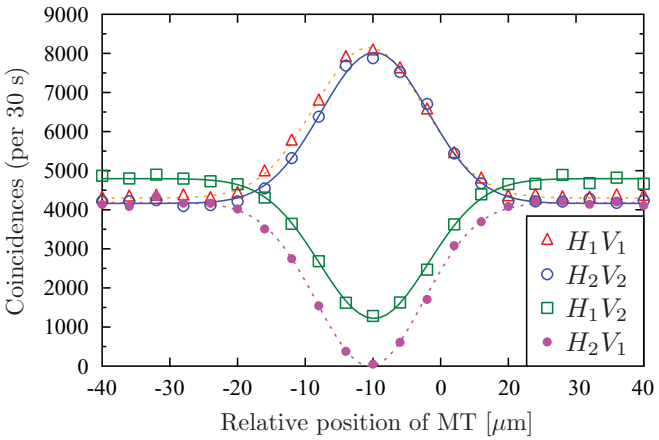

FIG. 2. (Color online) Coincidence measurement with the beam splitter BS2 shifted out to 0:100 position. Plotted are the measured coincidences H_1V_1, H_2V_2, H_1V_2, and H_2V_1 (markers) and their respective theoretical fits (lines). The relative position of the motorized translation MT has been set so that its origin corresponds to the center of H_2V_1 dip. Error bars are smaller than the marker size.

negligible (less than 150 coincidences per 30 s). Coincidence measurements have also been performed in the diagonal linear polarization basis. The observed dips in coincidence clicks of two detectors monitoring the same spatial mode are consistent with the absence of any $|2H, 0V\rangle$ or $|2V, 0H\rangle$ states. These measurements and the high fidelity of the input state with state $|\Phi_2\rangle$, which exhibits perfect anticorrelation of photon polarizations in the H-V basis, indicate that we can restrict ourselves to a three-dimensional Hilbert space spanned by the basis states $|H_1V_1\rangle$, $|H_2V_2\rangle$, $|H_1V_2\rangle$ when characterizing the generated KLM state.

In the second step of our analysis we verify the correct intensity ratios of H_1V_1, H_2V_2, and H_1V_2 terms. We have performed a series of coincidence measurements for different settings of parameter α to demonstrate the correct behavior of amplitudes γ and δ as functions of α. In Fig. 3(a) we plot the experimentally determined ratio of coincidences H_1V_1 and H_2V_2, showing that it approaches well the theoretical value of 1 in all cases. In Fig. 3(b) we plot the experimentally determined ratio of coincidences H_1V_1 and H_1V_2 together with the theoretical expectation γ^2/δ^2 given by Eq. (7). One may observe that the experimentally determined values correspond well to the theoretical prediction.

To fully analyze the prepared KLM state and determine its purity and fidelity one needs to perform a complete state tomography. For this purpose we employ the second beam splitter BS2 and thus form a Mach-Zehnder interferometer. The following three sets of coincidence measurements are carried out: First, we measure all coincidences (H_1V_1, H_2V_2, H_1V_2, H_2V_1) with beam splitter BS2 in the 0:100 position (a similar measurement as in the previous step). Second, we measure the same set of coincidences with BS2 in balanced position 50:50 ($\sigma = 1$) and with zero phase shift between the two arms of the interferometer. Finally, we measure with BS2 again in 50:50 position but with relative phase of $\frac{\pi}{4}$ between the two arms. The correct phase can be set using a piezo translation in one of the arms. This measurement requires us to perform two stabilization procedures: One is the stabilization

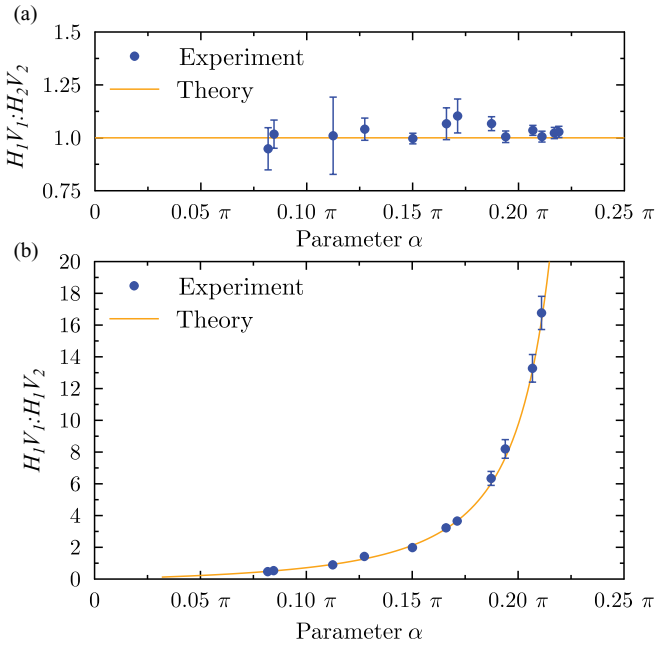

FIG. 3. (Color online) (a) Ratio of coincidences H_1V_1 and H_2V_2. (b) Ratio of coincidences H_1V_1 and H_1V_2. The experimental data with error bars are depicted by blue dots and the theoretical prediction according to Eq. (7) is plotted by the orange full line.

of the HOM dip on the first beam splitter BS1 and the second is the active stabilization of the phase in the interferometer. Dip stabilization is performed about every 30 s and MZ interferometer stabilization is carried out about every 5 s.

The three sets of measured coincidences provide sufficient data to fully reconstruct the density matrix of the generated

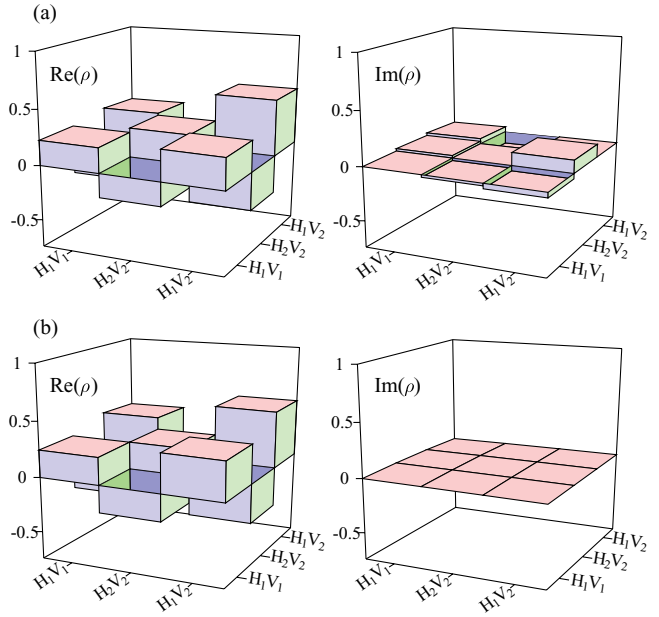

FIG. 4. (Color online) (a) Real and imaginary parts of reconstructed density matrix of KLM state with $\alpha = 0.08\pi$. (b) Theoretically determined density matrix of the corresponding pure target KLM state (2).

TABLE I. Purities and fidelities of three prepared KLM states with different parameters α. The purity P and fidelity of reconstructed state F is shown together with the fidelity F_C obtained after optimal compensation of local phase shifts.

α	γ^2/δ^2	P	F	F_C
0.17π	3.67	92.4%	93.5%	95.9%
0.11π	0.97	86.0%	91.1%	92.4%
0.08π	0.48	90.4%	92.9%	94.6%

KLM states. We have used the well-established maximum likelihood estimation method [22] and performed complete state tomography for three different KLM states (see Table I). Typical fidelities of prepared states are about 92% and purities about 90%. As an illustration we present one of the reconstructed density matrices as well as the related theoretical prediction in Fig. 4. Nonzero imaginary parts of reconstructed density matrix elements suggest that further improvement of the fidelity F can by achieved by application of local phase shifts, that is, by transformation $|H_1V_1\rangle \rightarrow |H_1V_1\rangle$, $|H_1V_2\rangle \rightarrow e^{i\theta_1}|H_1V_2\rangle, |H_2V_2\rangle \rightarrow e^{i\theta_2}|H_2V_2\rangle$. We have numerically determined the optimal phase shifts θ_1 and θ_2 that maximize the fidelity for a given reconstructed density matrix and target KLM state. We present the resulting improved fidelities F_C in the last column of Table I.

IV. CONCLUSIONS

In summary, we have presented a successful experimental preparation of two-photon KLM states using only SPDC photon source and linear optical components. The easy tunability of the entanglement source and of the splitting ratio of the beam splitter allows us to prepare any two-photon KLM state with fidelity of about 92% at the expense of losses on the beam splitter BS1 and therefore requiring postselection of cases when both photons arrive at detectors. These losses can however be overcome by employing a custom unbalanced beam splitter with splitting ratio calculated for some fixed value of α. In that way the scheme would not require any postselection, but it becomes limited to one specific KLM state corresponding to the splitting ratio of the chosen beam splitter.

ACKNOWLEDGMENTS

This research has been supported by the Ministry of Education of the Czech Republic under Project Nos. 1M06002, LC06007, MSM6198959213.

[1] G. Alber, T. Beth, and M. Horodecki, *Quantum Information* (Springer, Berlin, 2001).
[2] S. L. Braunstein and P. van Loock, Rev. Mod. Phys. **77**, 513 (2005).
[3] C. Benett and G. Brassard, in *IEEE International Conference on Computers, Systems, and Signal Processing* (1984).
[4] N. Gisin, G. Ribordy, W. Tittel, and H. Zbinden, Rev. Mod. Phys. **74**, 145 (2002).
[5] H.-K. Lo, X. Ma, and K. Chen, Phys. Rev. Lett. **94**, 230504 (2005).
[6] P. W. Shor, SIAM J. Sci. Stat. Comput. **26**, 1484 (1997).
[7] A. Ekert and R. Jozsa, Rev. Mod. Phys. **68**, 733 (1996).
[8] D. S. Abrams and S. Lloyd, Phys. Rev. Lett. **83**, 5162 (1999).
[9] N. Shenvi, J. Kempe, and K. Birgitta Whaley, Phys. Rev. A **67**, 052307 (2003).
[10] D. Bowmeester, A. Ekert, and A. Zeilinger, *The Physics of Quantum Information* (Springer, Berlin, 2000).
[11] E. Knill, R. Laflamme, and G. Milburn, Nature (London) **409**, 46 (2001).
[12] P. Kok, W. J. Munro, K. Nemoto, T. C. Ralph, J. P. Dowling, and G. J. Milburn, Rev. Mod. Phys. **79**, 135 (2007).
[13] J. D. Franson, M. M. Donegan, M. J. Fitch, B. C. Jacobs, and T. B. Pittman, Phys. Rev. Lett. **89**, 137901 (2002).
[14] J. O'Brien, G. Pryde, A. White, T. Ralph, and D. Branning, Nature (London) **426**, 264 (2003).
[15] A. Černoch, J. Soubusta, L. Bartušková, M. Dušek, and J. Fiurášek, Phys. Rev. Lett. **100**, 180501 (2008).
[16] B. P. Lanyon, M. Barbieri, M. P. Almeida, T. Jennewein, T. C. Ralph, K. J. Resch, G. J. Pryde, J. L. O'Brien, A. Gilchrist, and A. G. White, Nat. Phys. **5**, 134 (2009).
[17] A. Černoch, L. Bartušková, J. Soubusta, M. Ježek, J. Fiurášek, and M. Dušek, Phys. Rev. A **74**, 042327 (2006).
[18] T. B. Pittman, B. C. Jacobs, and J. D. Franson, Phys. Rev. A **64**, 062311 (2001); **71**, 032307 (2005).
[19] J. Modlawska and A. Grudka, Phys. Rev. Lett. **100**, 110503 (2008); Phys. Rev. A **79**, 064302 (2009); A. Grudka and J. Modlawska, *ibid.* **77**, 014301 (2008).
[20] K. Lemr and J. Fiurášek, Phys. Rev. A **77**, 023802 (2008).
[21] P. G. Kwiat, E. Waks, A. G. White, I. Appelbaum, and P. H. Eberhard, Phys. Rev. A **60**, R773 (1999).
[22] M. Ježek, J. Fiurášek, and Z. Hradil, Phys. Rev. A **68**, 012305 (2003).
[23] C. K. Hong, Z. Y. Ou, and L. Mandel, Phys. Rev. Lett. **59**, 2044 (1987).